Moving Objects Segmentation Using Optical Flow Estimation

F. Ranchin, F. Dibos*
CEREMADE (URA CNRS 749), Université Paris 9 – Dauphine,
Place du Maréchal De Lattre De Tassigny,
75775 Paris cedex 16, France

18th June 2004

Abstract

In this paper, we present a new method for the segmentation of moving objects. We use one of the most powerful variational method for computing the optical flow and we exploit this information in the segmentation. This segmentation lies on well-known techniques of active contours.
Since we can distinguish moving objects from static elements of a scene by analyzing norm of the optical flow vectors, this one is incorporated in a region-based active contour model in order to attract the evolving contour to moving objects contours. We also take gray level into account since it is known that optical flow information does not give the exact contours of the objects.
The results provided are promising and extend the numerous works on this subject.

Keywords: Segmentation, edge and feature detection.

1 Introduction

Segmentation of moving objects from a video sequence is an important task whose applications cover domains such like video compression, video surveillance or object recognition. In video compression, the MPEG-4 video coding standard is based on the representation of the scene as different shapes-objects. This representation symplify the scene and is used for the encoding of the sequence.
There are different ways to perform moving objects segmentation, using different mathematical techniques. For Markov Random Fields based methods, we refer to the works of Bouthemy ([BL], [PHB]) and for maximum likelihood based methods, to the works of Deriche and Paragios ([DP]). For variational techniques, we refer to the works of Deriche *et al.* ([ADK]) and Barlaud *et al.* ([ABJB]). At last, mathematical morphology has been more and more used these last ten years, see the works

*{fd,ranchin}@ceremade.dauphine.fr

of Salembier, Serra and their teams ([BCJM]).

Our aim is to discriminate moving objects from a static background. This is not restrictive since the seminal work of Odobez and Bouthemy ([OB]), one can compute the 2D parametric motion (euclidean, affine, ...) which approaches mostly well a true projective camera motion. Thus, we will not consider segmentation of piecewise constant or affine motion as in the works of Cremers (see [Cre] for example).
Since we use optical flow magnitude, one could claim we do not use all the information and in particular the optical flow direction is not used. However, using optical flow direction imposes first to threshold the magnitude at a positive level before any computation since the direction is no more reliable for low magnitude vectors, thus we have to tune this threshold. Secondly, given a good threshold, we should take the magnitude into account, since giving an equal weight to vectors of same directions but with very different magnitudes could be sensitive. In [ABDR], Aubert, Barlaud, Debreuve and Roy have proposed a directional vector field segmentation, but it uses only the direction. Another way to use the direction is to apply a piecewise constant Mumford-Shah multichannel segmentation as in [SD]. These are at our knowledge the only works about vector field segmentation using the direction information.
So we need to compute the velocity of each point in the image. The most employed tool for computing the apparent motion from a video sequence is the optical flow. Computation of the optical flow can be achieved by many different methods, among a large litterature, we can cite the pioneer work of Horn and Schunck [HS], the works of Aubert, Deriche and Kornprobst [ADK] and Weickert and Schnörr [WS]; there are also tensor-based methods such like in [LK] or [BGW]. In this work, we compute the optical flow by one of the most popular technique, then we use the norm of the optical flow as an input in an active contour model. So we will first present the Weickert-Schnörr optical flow estimation and compare the quality of the results in terms of magnitude, then we will introduce our model. At last, we recall the techniques for the derivation of shape functionals in appendix.

2 Optical Flow Estimation

Variational methods are based on the assumption of spatial smoothness of the optical flow. That means regularization terms in the energy depend on the spatial gradient of the optical flow. The idea of Weickert and Schnörr is to replace the spatial gradient $\nabla = \left(\frac{\partial}{\partial x}\ \frac{\partial}{\partial y}\right)^T$ of the optical flow by the spatio-temporal gradient $\nabla^\theta = \left(\frac{\partial}{\partial x}\ \frac{\partial}{\partial y}\ \frac{\partial}{\partial t}\right)^T$, leading to a spatio-temporal smoothness constraint. The energy to be minimized is

$$E(\mathbf{v}) = \int_{\Omega\times[0,T]} |\nabla I \cdot \mathbf{v} + I_t|^2 \, dx\, dy\, dt + \alpha \int_{\Omega\times[0,T]} \Psi(|\nabla^\theta v_1|^2 + |\nabla^\theta v_2|^2)\, dx\, dy\, dt$$

where $\mathbf{v} = (v_1, v_2)$ is the optical flow and Ψ is one of the function classically used to smooth the data with keeping its discontinuities, for example $\Psi(s^2) = \epsilon s^2 + (1 -$

$\epsilon)\lambda^2\sqrt{1+\frac{s^2}{\lambda^2}}$. The parameter ϵ garantees the well-posedness of the minimization problem. The Euler-Lagrange equations for the minimization problem give

$$\begin{aligned} 0 &= -I_x(I_x v_1 + I_y v_2 + I_t) + \tfrac{1}{\alpha}\mathrm{div}\left(\psi'(|\nabla^\theta v_1|^2 + |\nabla^\theta v_2|^2)\nabla^\theta v_1\right) \\ 0 &= -I_y(I_x v_1 + I_y v_2 + I_t) + \tfrac{1}{\alpha}\mathrm{div}\left(\psi'(|\nabla^\theta v_1|^2 + |\nabla^\theta v_2|^2)\nabla^\theta v_2\right). \end{aligned}$$

Experimentally, the assumption of spatio-temporal smoothness reduces significantly the amount of noise in the flow in comparison with spatial smoothness-based optical flow determination.
As we use the optical flow as an input of our segmentation model, the result will naturally depend on the quality of the optical flow. To overcome well-known difficulties in optical flow determination, we have embedded the Weickert and Schnörr algorithm with a multiresolution procedure.

1. We start from a coarse (downsampled) version I^J of the image I at the resolution J (the finest resolution is taken as 0). Then we solve the minimization of E to find $\mathbf{v}^J$.

2. For the resolution $j < J$, we use the optical flow determined at the resolution $j+1$ by searching the residue $\mathbf{w}^j = \mathbf{v}^j - T\mathbf{v}^{j+1}$ (T is an oversampling operator which constructs the image of $\mathbf{v}^{j+1}$ on the grid at the resolution j). In the time derivative of I, we replace the image by itself compensated by the motion $T\mathbf{v}^{j+1}$
$$\tilde{I_t^j}(\mathbf{x}, t) = I^j(\mathbf{x}, t+1) - I^j(\mathbf{x} - T\mathbf{v}^{j+1}, t).$$

3. Then we iter this procedure from $j = J$ to $j = 0$.

Introduced by Mémin and Pérez in [MP], this procedure allows to overcome the locality problem of the optical flow, that is to say one cannot determine it correctly when displacements are larger than the size of the mask used for the approximation of the gradient. In our case, it is also a good way to avoid too weak optical flow values in very homogeneous zones where $|\nabla I| \approx 0$ in choosing a suitable value for the regularization parameter α. Thus the moving objects are quite well filled even they contain homogeneous zones.

In [KWSR], Weickert and his collaborators use a tensor-based optical flow determination which was introduced by Bigün *et al.* in [BGW]. This method relies on the fact that the optical flow is constant on a neighborhood of each pixel. The optical flow constraint

$$I_x u + I_y v + I_t = 0$$

can be rewritten as $< \nabla^\theta I, (u\ v\ 1)^T >= 0$. Then they minimize the energy

$$\frac{1}{2}\int_{\mathcal{V}(x_0,y_0,t_0)} | < \nabla^\theta I, (u\ v\ 1)^T > |^2\, dx\, dy\, dt,$$

which is quite straightforward since the optical flow is constant over $\mathcal{V}(x_0, y_0, t_0)$; the solution is given by the eigenvector corresponding to the minimum eigenvalue of the *structure tensor*

$$S(\mathcal{V}(x_0, y_0, t_0)) = \int_{\mathcal{V}(x_0,y_0,t_0)} \nabla^\theta I (\nabla^\theta I)^T\, dx\, dy\, dt$$

Then, the authors of [KWSR] use the *coherence* measures $c_t = \exp(-\frac{C}{|\lambda_1 - \lambda_3|})$ and $c_s = \exp(-\frac{C}{|\lambda_2 - \lambda_3|})$. If they are both sufficiently near from 1 ($c_t > 1-\epsilon$ and $c_s > 1-\epsilon$), optical flow can be reliably computed.
However this method fails if the moving objects have a too little size in comparison to the size of the neighborhood chosen. Increasing the size of the neighborhood reduces noise but it imposes a sufficiently large size of the moving objects. In the example shown below, some cars are too small for the size of neighborhood $|\mathcal{V}| = 7^3$ pixels (7^2 pixels on 7 successive frames) which seems to be the best choice for noise reducing, and the quality of the optical flow is not too good. This disadvantage may be avoided by performing anisotropic filtering of the tensor $\nabla^\theta I (\nabla^\theta I)^T$, but in [BW], Weickert and his collaborators have made a comparison between many optical flow algorithms, including tensor-based methods relying on a tensor anisotropic presmoothing. The conclusion is that the Weickert and Schnörr algorithm gives a better result for the average angular error than any other.
On the FIG. 1, we present some results of optical flow magnitude thresholding. For the Horn and Schunck method (the same model than Weickert and Schnörr's one, except there is no integration over time and $\Psi(s^2) = s^2$), the number of iterations was of $N = 500$ and the regularizing parameter of 4. The Weickert and Schnörr computation, we have fixed the iteration number to $N = 150$, the time step to $\Delta t = \frac{1}{6}$, $\epsilon = 10^{-5}$ and $\alpha = 750$. For the tensor-based method with coherence measures, we used $C = 5$ and $\epsilon = 0.25$. Of course, the Horn and Schunck result is extremely noisy since we have chosen a quite weak value of α; on the other hand, increasing α would lead to an edge smoothing and worse results on the moving objects. Visually, the Weickert and Schnörr method with multiresolution (3 levels for the pyramid) gives the best results and fills quite well homogeneous zones (see the car in the bottom left of the image). This has lead us to keep it for our segmentation algorithm.

3 A region-based active contour model

Active contour models have been introduced first by Kass, Witkin and Terzopoulos in [KWT]. A parametrized curve is searched as the solution of the minimization problem

$$J_{KWT}(\Gamma) = \int_0^{L(\Gamma)} -|\nabla I(\Gamma(s))|^2 \, ds + C \int_0^{L(\Gamma)} (a + |\kappa(s)|^2) \, ds.$$

The first term helps to attract the curve towards high gradient values of the image, *i.e.* the edges, while the last integral garantees the smoothness of the curve (it has a finite perimeter and a finite total curvature). Unfortunately, this model does not allow the curve break since the curve is parametrized and the smoothness is controlled by the last integral.
In [CCCD], Caselles, Catté, Coll and Dibos have introduced a *snake* model that allows topology changes. The curve is represented as the zero level set of a function u that is evolved by the PDE

$$\frac{\partial u}{\partial t} = g(|\nabla G_\sigma I|)|\nabla u| \left(\text{div} \left(\frac{\nabla u}{|\nabla u|} \right) + \nu \right) \tag{1}$$

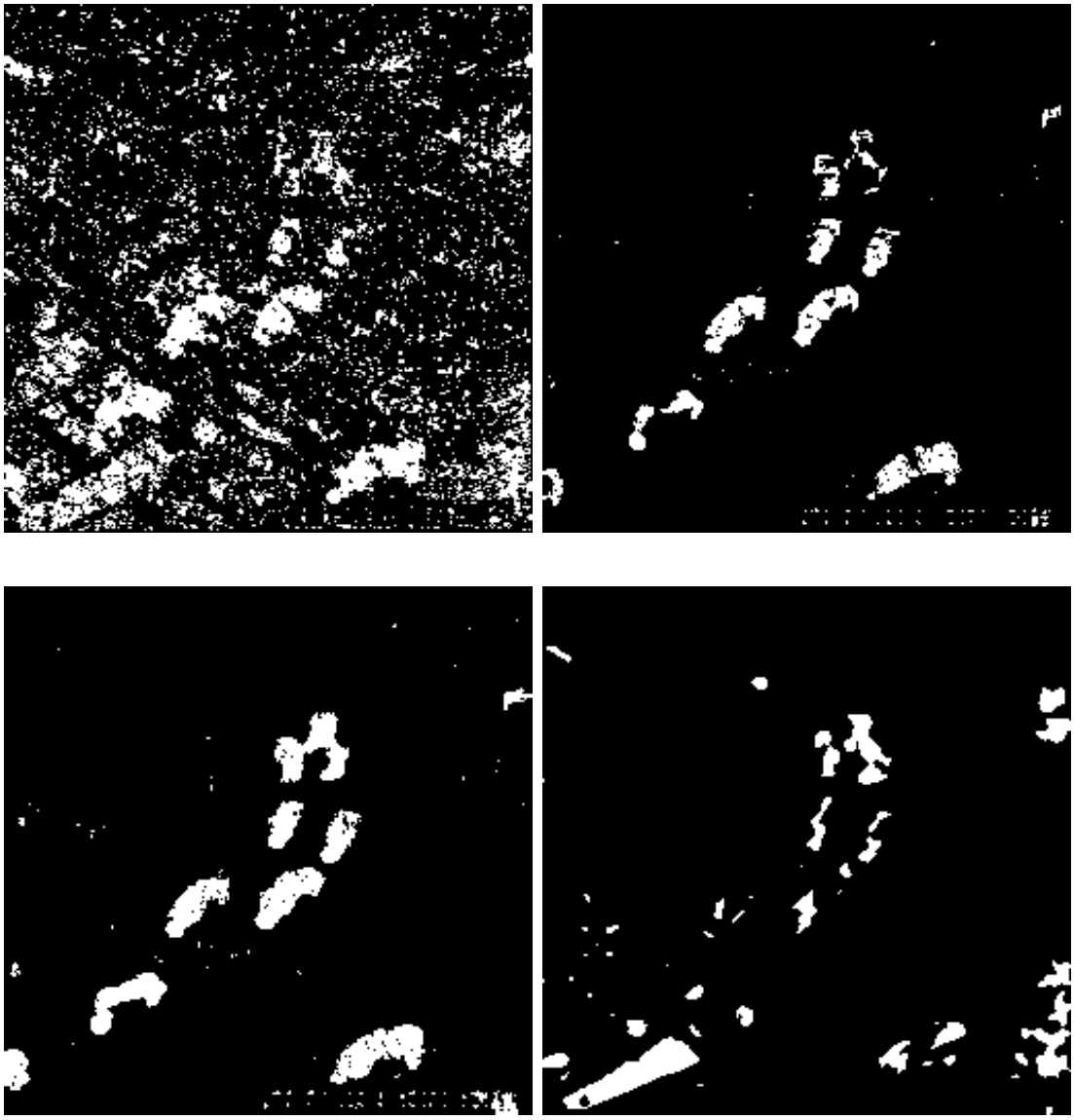

FIG. 1: Results of a thresholding of the optical flow norm on the 10th frame of the sequence. From left to right and top to bottom: Horn and Schunck, Weickert-Schnörr, Weickert-Schnörr with multiresolution and Bigün tensor-based method. The three first ones are thresholded at level 0.7 and the last one at 0.5.

where $g(r) = \frac{1}{1+r^2}$, ν is a parameter chosen such that non convex contours may be obtained. This is a level set model inspired from the level sets methods introduced by Osher and Sethian [OS] and so allows topology changes, that is to say that the curve can split into several Jordan curves during his evolution.
Contour-based segmentation is a difficult task if we use the optical flow as an input of our video segmentation. In [KWSR], Weickert *et al.* use geodesic active contours, but the function g used is the characteristic function based on the coherence function $c_t = \exp(-\frac{1}{|\lambda_1 - \lambda_3|})$ (λ_1 and λ_3 are the extremal eigenvalues of the structure tensor $\int_{\mathcal{V}} \nabla^\theta I (\nabla^\theta I)^T \, d\mathbf{x}$) and the optical flow norm $|\mathbf{v}|$

$$g = \mathbf{1}(c_t(x,y) > 1 - \epsilon \text{ and } |\mathbf{v}| > \alpha)$$

where ϵ and α are two given parameters. Such a function is more related to a region information, as a consequence, the idea to incorporate region information from the inside and outside regions seems more natural than using this function as a boundary potential.
What we want to do is to have the optical flow norm upper a certain threshold on the inside region and lower on the outside region. In addition, we would like the boundary be an edge of the image I. The most natural way to realize this is to minimize the function $g(|\nabla G_\sigma I|)$ along the boundary with $g(r) = \frac{1}{1+r^2}$. Unfortunately, we have seen that this is not sufficient to provide a segmentation of good quality and produces irregular contours. That is the reason why we have added a term penalizing the curve length. For notation simplicity , we will denote $g(|\nabla G_\sigma I(\mathbf{x})|)$ by $g(\mathbf{x})$. Finally, we minimize the functional

$$E(\Omega) = \int_\Omega \alpha \, d\mathbf{x} + \int_{D \setminus \Omega} |\mathbf{v}| \, d\mathbf{x} + \lambda \int_{\partial\Omega} g(\mathbf{x}) \, d\mathcal{H}^1(\mathbf{x}) + \nu \int_{\partial\Omega} d\mathcal{H}^1(\mathbf{x}).$$

Using either shape sentivity analysis or heaviside functions techniques, we obtain

$$dE(\Omega; V) = \int_{\partial\Omega} (\alpha - |\mathbf{v}| + (\lambda g + \nu)\kappa + \lambda < \nabla g, \mathbf{n} >) < V, \mathbf{n} > \, ds$$

or

$$dE_\epsilon(u; v) = \int_D \left(\alpha - |\mathbf{v}| - (\lambda g + \nu) \text{div} \left(\frac{\nabla u}{|\nabla u|} \right) - \lambda < \nabla g, \frac{\nabla u}{|\nabla u|} > \right) \delta_\epsilon(u) v \, d\mathbf{x}$$

respectively.

The minimization of the energy E can be achieved by a gradient descent method on the contour by choosing in the direction V as $-\left((\lambda g(\mathbf{x}) + \nu)\kappa + \lambda < \nabla g, \mathbf{n} > + \alpha - |\mathbf{v}|\right) \mathbf{n}$

$$\frac{\partial \Gamma}{\partial t} = -\left((\lambda g(\mathbf{x}) + \nu)\kappa + \lambda < \nabla g, \mathbf{n} > + \alpha - |\mathbf{v}|\right) \mathbf{n}. \tag{2}$$

If we use the energy E_ϵ, the minimization is achieved by taking v as
$-\left(\alpha - |\mathbf{v}| - (\lambda g + \nu) \text{div} \left(\frac{\nabla u}{|\nabla u|} \right) - \lambda < \nabla g, \frac{\nabla u}{|\nabla u|} > \right) \delta_\epsilon(u)$, leading to the PDE

$$\frac{\partial u}{\partial t} = \delta_\epsilon(u) \left(\text{div} \left((\lambda g(\mathbf{x}) + \nu) \frac{\nabla u}{|\nabla u|} \right) + |\mathbf{v}| - \alpha \right). \tag{3}$$

3.1 Analysis of the different terms in the energy and experimental results

We recall that we minimize

$$E(\Omega) = \int_{\Omega} \alpha \, d\mathbf{x} + \int_{D\setminus\Omega} |\mathbf{v}| \, d\mathbf{x} + \lambda \int_{\partial\Omega} g(\mathbf{x}) \, d\mathcal{H}^1(\mathbf{x}) + \nu \int_{\partial\Omega} d\mathcal{H}^1(\mathbf{x}).$$

Let us comment on this energy.

- The first term is an area term since it is $\alpha|\Omega|$. As we increase α, we minimize more and more the area of the domain, so it should contain few connex components of weak areas, that is to say few noise, as we can assimilate these regions to noise. How to choose it remains in our case a difficult problem. We could do adaptive thresholding (choosing different thresholds and apply the algorithm for each of them using the result for the previous threshold as initialization), as proposed in [JB], but as we decrease α, we extend also the regions enclosing the moving objects and we lose precision, even if the objects are more filled. Thus we have not applied this and have chosen visually α.

- Minimizing the second term simply implies that the optical flow norm is not too high on the complementary domain of Ω.

- The third term is simply an edge potential that helps the contours to be attracted by the real edges of the image. In order to significantly take the gray level into account, we have to tune the parameter λ to balance the first two terms.

- The fourth term is a length term which gives more regularity to the contours. The higher ν is, the more regular the contour will be, as it tends to minimize the length of the curves.

One could claim our model is quite the same as the one proposed by Aubert, Barlaud and Jehan-Besson in [ABJB], where these authors minimize

$$E_{ABJB}(\Omega) = \int_{\Omega} \alpha \, d\mathbf{x} + \int_{D\setminus\Omega} |B - I| + \nu \int_{\partial\Omega} d\mathcal{H}^1(\mathbf{x}),$$

where I is the image on which we detect moving areas and B is a background computed by any method of background computation, the simplest and the fastest is the time median filter. The PDE obtained by gradient descent can be simply expressed

$$\frac{\partial u}{\partial t} = \delta_\epsilon(u) \left(\nu \mathrm{div}\left(\frac{\nabla u}{|\nabla u|} \right) + |B - I| - \alpha \right).$$

We present a result of this method on FIG. 2. The background computed by temporal median filter is of good quality, the objects are sufficiently contrasted from the background, then the segmentation is visually excellent.

The difference of our model lies in the mixture of the gray level information via the edge potential with the optical flow information. We present in FIG. 3 some results which tend to prove the edge potential is useful to separate objects not separated by optical flow information. Thus we do not claim the edge potential is absolutely

FIG. 2: On the left:background image computed by temporal median filter, on the right:result for the Aubert, Barlaud and Jehan-Besson model ($\alpha = 20$, $\nu = 10$, time step $\Delta t = 5$).

crucial, the main reason of its introduction in the functional being our segmentation would not be based on gray level information if we have not introduced it. On FIG. 4, we show the length term is very important since the contours are quite irregular if we keep only the edge potential. At last, the crucial question that we have to address here is to compare the mask obtained by thresholding $|\mathbf{v}|$ at the level α (which is used as the initialization of our algorithm) and the mask obtained by our algorithm. This is shown on FIG. 6 where $\alpha = 0.7$. We can see that the mask is well denoised (even if there remains some noise on the post) and that the edge potential is not awkward since we have the length term:if we can recognize some very noisy geometric features (the ground marks), they are not retrieved by our algorithm which is correct since they are not in motion.

A Shape sensitivity analysis

For the derivation of energies depending on a shape, we need the notion of shape derivatives. This was introduced by Sokolowski and Zolésio in [SZ]. Following [SZ], we consider a transformation $T_t(V) : \mathbf{x} \to \mathbf{X}(t)$, $\mathbf{X}(t)$ being given as the solution of the ordinary differential equation (V is a smooth vector field with compact support)

$$\left\{ \begin{array}{rcl} \mathbf{X}'(t) & = & V(\mathbf{X}(t)) \\ \mathbf{X}(0) & = & \mathbf{x}. \end{array} \right. \tag{4}$$

Then, the images of the shape Ω and its boundary Γ by the transformation $T_t(V)$ are simply defined as

$$\begin{array}{rcl} \Gamma_t & = & \{T_t(V)(\mathbf{x}),\, \mathbf{x} \in \Gamma\} = T_t(V)(\Gamma) \\ \Omega_t & = & \{T_t(V)(\mathbf{x}),\, \mathbf{x} \in \Omega\} = T_t(V)(\Omega). \end{array}$$

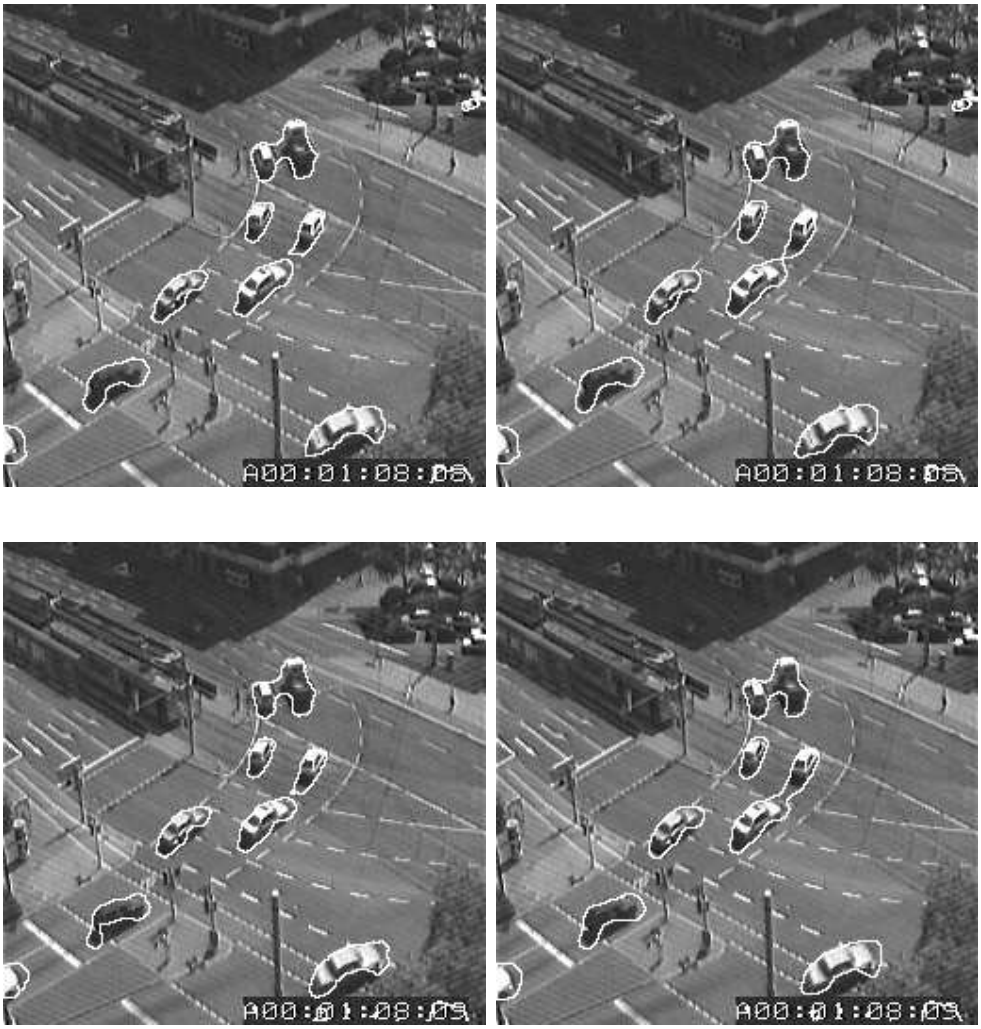

FIG. 3: Result of our method with (left images) and without (right images) the edge potential term. The parameters are $\alpha = 0.6$, $\nu = 2$, $\lambda = 100$, $\epsilon = 1.5$ and $\Delta t = 0.01$ for the time step. The initialization for the algorithm is chosen as the signed distance function to the mask obtained by thresholding the optical flow magnitude at the level α. See the separation between the two cars in the middle of the image with the edge potential.

FIG. 4: Result of our method with (left images) and without (right images) the length term. The parameters are $\alpha = 0.6$, $\nu = 2$, $\lambda = 100$, $\epsilon = 1.5$ and $\Delta t = 0.01$ for the time step. The initialization for the algorithm is chosen as the signed distance function to the mask obtained by thresholding the optical flow magnitude at the level α. Compare the irregularity of the contours on the right image with the smooth ones on the left image.

From these preliminaries, the *Eulerian* shape derivative of a function $J(\Omega)$ (*resp.* $J(\Gamma)$) is defined as

$$dJ(\Omega; V) = \lim_{t \downarrow 0} \frac{1}{t} \left(J(\Omega_t) - J(\Omega) \right) \left(resp.\ dJ(\Gamma; V) = \lim_{t \downarrow 0} \frac{1}{t} \left(J(\Gamma_t) - J(\Gamma) \right) \right) \tag{5}$$

From Sokolowski and Zolésio works, we will use the following theorem

Theorem 1 *The cost functional*

$$J(\Omega) = \int_{\Omega} \phi(\mathbf{x})\, d\mathbf{x} \tag{6}$$

is shape differentiable and we have

$$dJ(\Omega; V) = \int_{\Gamma} \phi < V, \mathbf{n} > \, d\mathcal{H}^1(\mathbf{x}). \tag{7}$$

Under similar hypothesis, for a cost functional

$$J(\Gamma) = \int_{\Gamma} \psi(\mathbf{x})\, d\mathcal{H}^1(\mathbf{x}) \tag{8}$$

the shape derivative exists and is given by

$$dJ(\Gamma; V) = \int_{\Gamma} \left(\kappa \psi + \frac{\partial \psi}{\partial n} \right) < V, \mathbf{n} > \, d\mathcal{H}^1(\mathbf{x}) \tag{9}$$

where κ denotes the curvature of Γ and $\mathbf{n}$ its outward normal.

Let us note that a more general theorem could be formulated about the same functionals when the functions ϕ and ψ depend also on the shape Ω (*resp.* Γ) itself. We refer to [SZ] and [DeZo] for this case.

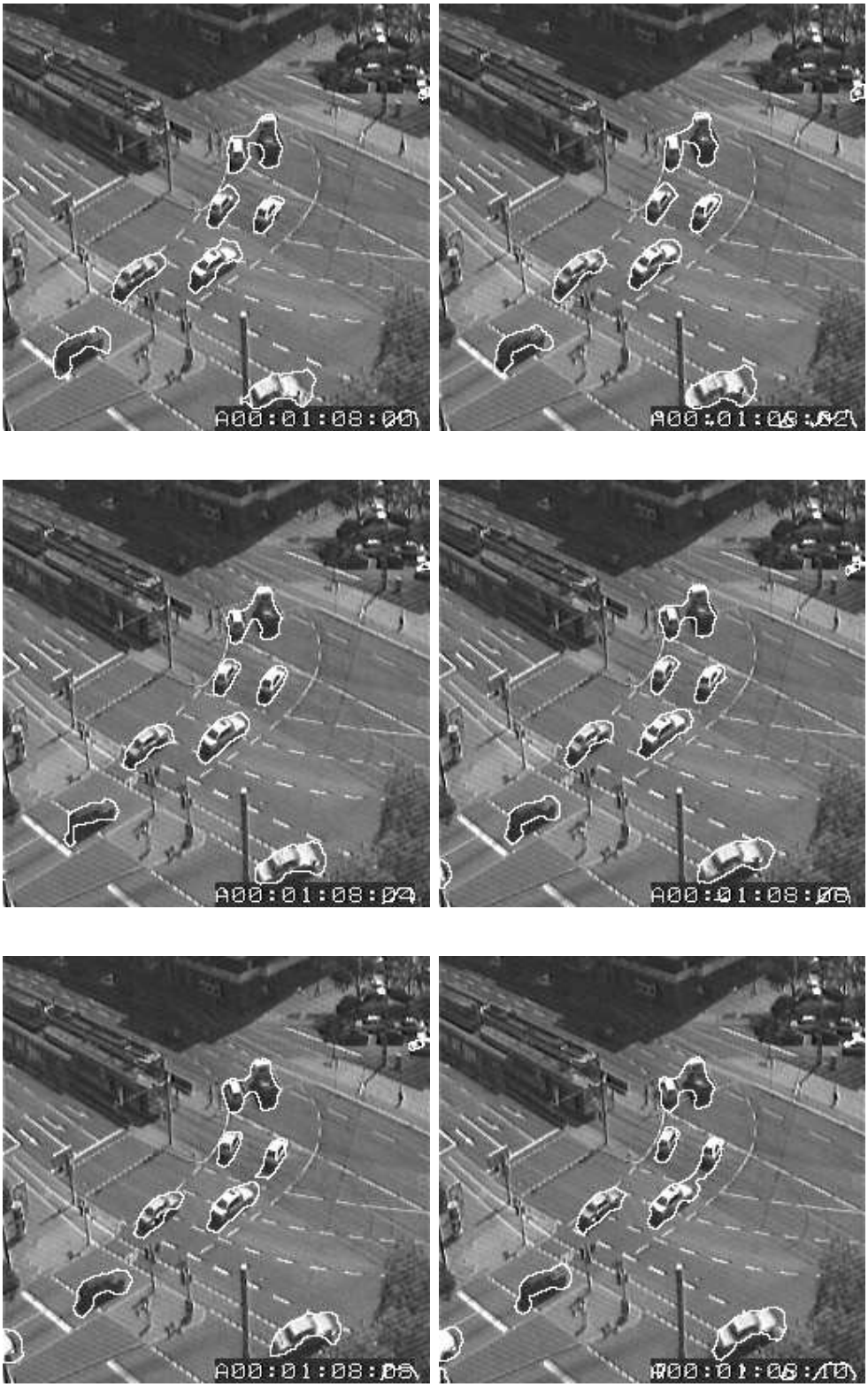

FIG. 5: Results for our model on even images of the sequence. The parameters are $\alpha = 0.6$, $\nu = 2$, $\lambda = 100$, $\epsilon = 1.5$ and $\Delta t = 0.01$ for the time step.

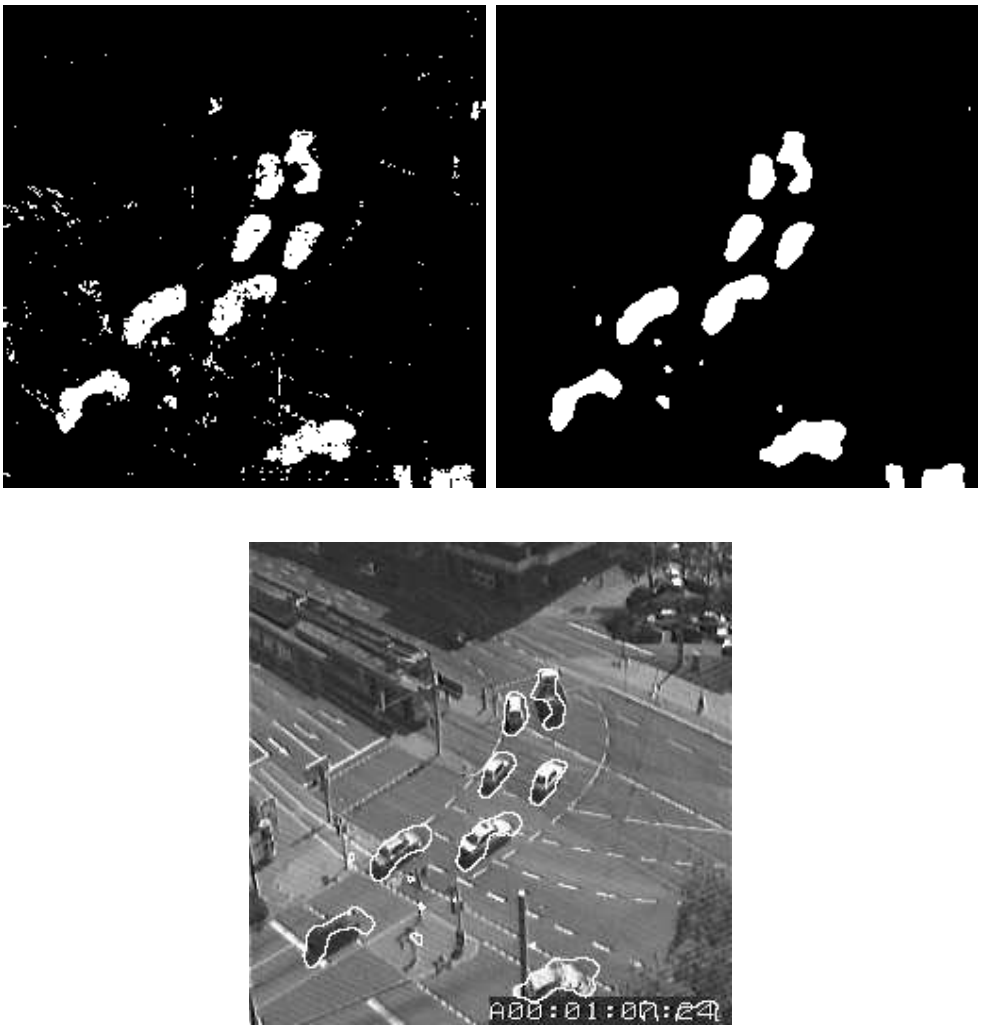

FIG. 6: Successively (from left to right and top to bottom): the initial mask (optical flow magnitude thresholded at level 0.7, the resulting mask of our algorithm) for the parameters $\alpha = 0.7$, $\nu = 2$, $\lambda = 100$, $\epsilon = 1.5$, $\Delta t = 0.01$; the mask superimposed to the image.

B Technique of heaviside functions

In their seminal work [CV], Chan and Vese have introduced a new method for the representation and the derivation of a shape functional $J(\Omega)$. Following Osher and Sethian ([OS]), they represent Ω as the set of positive values of a function u

$$\Omega = \{\mathbf{x}|\, u(\mathbf{x}) > 0\} = \{\mathbf{x}|\, H(u(\mathbf{x})) = 1\} = \lim_{\epsilon\to 0}\{\mathbf{x}|\, H_\epsilon(u(\mathbf{x})) = 1\}$$

and

$$\partial\Omega = \{\mathbf{x}|\, u(\mathbf{x}) = 0\} = \{\mathbf{x}|\, \delta(u(\mathbf{x})) = +\infty\} = \lim_{\epsilon\to 0}\{\mathbf{x}|\, \delta_\epsilon(u(\mathbf{x})) = \frac{1}{\epsilon}\},$$

where $H_\epsilon(s) = 1 + \frac{2}{\pi}\arctan(\frac{s}{\epsilon})$ and $\delta_\epsilon(s) = \frac{2}{\pi}\frac{\epsilon}{\epsilon^2+s^2}$ are C^∞ approximations of the Heaviside and Dirac distributions.
Then the general functional

$$J(\Omega) = \int_\Omega k_{in}(\mathbf{x},\Omega)\, d\mathbf{x} + \int_{\Omega^c} k_{out}(\mathbf{x},\Omega^c)\, d\mathbf{x} + \int_{\partial\Omega} k_b(\mathbf{x})\, d\mathcal{H}^1(\mathbf{x})$$

is replaced by

$$J_\epsilon(u) = \int_D k_{in}(\mathbf{x},u)H_\epsilon(u(\mathbf{x}))\, d\mathbf{x} + \int_D k_{out}(\mathbf{x},u)(1 - H_\epsilon(u(\mathbf{x})))\, d\mathbf{x} + \int_D k_b(\mathbf{x})\delta_\epsilon(u(\mathbf{x}))|\nabla u|\, d\mathbf{x}.$$

This functional can be derived using the classical way:we compute the Gâteaux derivative in the direction v as the limit of $\frac{J_\epsilon(u+tv)-J_\epsilon(u)}{t}$ and we obtain

$$dJ(u;v) = \int_D \partial_2 k_{in}(\mathbf{x},u)H_\epsilon(u)v\, d\mathbf{x} + \int_D \partial_2 k_{out}(\mathbf{x},u)(1 - H_\epsilon(u))v\, d\mathbf{x} + \int_D \left(k_{in} - k_{out} - \left(k_b \operatorname{div}\left(\frac{\nabla u}{|\nabla u|}\right) + \nabla k_b \cdot \frac{\nabla u}{|\nabla u|}\right)\right)\delta_\epsilon(u)v\, d\mathbf{x}$$

References

[ADK] **G. Aubert, R. Deriche and P. Kornprobst**, *Image Sequence Analysis via Partial Differential Equations*, Journal of Mathematical Imaging and Vision **11 1** (1999), 5-26;

[ABDR] **G. Aubert, M. Barlaud, E. Debreuve and T. Roy**, *Vector Field Segmentation Using Active Contours : Regions Of Vectors With The Same Direction*, Proceedings of the 2nd IEEE Workshop on Variational, Geometric and Level Set Methods in Computer Vision (2003);

[ABJB] **G. Aubert, M. Barlaud and S. Jehan-Besson**, *Video Object Segmentation Using Eulerian Region-Based Active Contours*, International Conference in Computer Vision (2001), Vancouver, Canada;

[BGW] **J. Bigün, G. H. Granlund and J. Wiklund**, *Multidimensional Orientation Estimation with Applications to Texture Analysis and Optical Flow*, IEEE Transactions on Pattern Analysis and Machine Intelligence **n° 8** (1991), 775-790;

[BCJM] **L. Bouchard, I. Corset, S. Jeannin, F. Marqués, F. Meyer, R. Morros, M. Pardàs, B. Marcotegui and P. Salembier**, *Segmentation-based Video Coding System Allowing the Manipulation of Objects*, IEEE Transactions on Circuits and Systems for Video Technology, (RACE/MAVT and MORPHECO Projects) **7 n° 1** (1997), 60-74;

[BL] **P. Bouthemy and P. Lalande**, *Recovery of Moving Object Masks in an Image Sequence Using Local Spatiotemporal Contextual Information*, Optical Engineering **32 n° 6** (1993), 1205-1212;

[BW] **T. Brox and J. Weickert**, *Nonlinear Matrix Diffusion for Optic Flow Estimation*, Proceedings 24th DAGM Symposium, Springer LNCS 2449 (L. Van Gool, eds.) (2002), 446-453;

[CCCD] **V. Caselles, F. Catté, B. Coll and F. Dibos**, *A Geometric Model for Active Contours in Image Processing*, Numerische Mathematik **66** (1993), 1-31;

[KWT] **M. Kass, A. Witkin and D. Terzopoulos**, *Snakes : Active Contour Models*, International Journal of Computer Vision **1** (1988), 321-332;

[PHB] **P. Bouthemy, F. Heitz and P. Perez**, *Multiscale Minimization of Global Energy Functions in Some Visual Recovery Problems*, CVGIP : Image understanding **59 n° 1** (1989), 191-212;

[CV] **T. F. Chan and L. A. Vese**, *Active Contours without Edges*, IEEE Transactions on Image Processing **10(2)** (2001), 266-277;

[Cre] **D. Cremers**, *A Multiphase Level Set Framework for Motion Segmentation*, Proceedings of the 4th Int. Conf. on Scale-Space Theories in Computer Vision Proceedings, Springer LNCS (L.D. Griffin and M. Lillholm, eds.) **2695** (2003), 599-614;

[CS] **D. Cremers and C. Schnörr**, *Motion Competition : Variational Integration of Motion Segmentation and Shape Regularization*, Proceedings of the German Conf. on Pattern Recognition (DAGM), Springer LNCS (L. Van Gool, eds.) **2449** (2002), 472-480;

[DeZo] **M. Delfour and J.-P. Zolésio**, SHAPES AND GEOMETRIES, SIAM, Philadelphia, PA, Advances in Design and Control, 2001;

[DP] **R. Deriche and N. Paragios**, *Geodesic Active Regions for Motion Estimation and Tracking*, INRIA Research Report n° 3631 (1999);

[HS] **B.K.P. Horn and B. Schunck**, *Determinating Optical Flow*, Artificial intelligence (1981);

[JB] **S. Jehan-Besson**, *Modèles de contours actifs basés régions pour la segmentation d'images et de vidéos*, Ph.D. thesis (2003);

[KWSR] **G. Kühne, J. Weickert, O. Schuster, S. Richter**, *A Tensor-Driven Active Contour Model for Moving Object Segmentation*, IEEE Proceedings on International Conference on Image Processing **2** (2001), 73-76;

[LK] **B. Lucas and T. Kanade**, *An Iterative Image Registration Technique with an Application to Stereo Vision*, International Joint Conference on Artificial Intelligence (1981), 674-679;

[MP] **E. Mémin and P. Perez**, *A Multigrid approach for hierarchical motion estimation*, Proceedings of the 6th International Journal of Computer Vision, IEEE Computer Society Press (1998), 933-938;

[OB] **J.-M. Odobez and P. Bouthemy**, *Robust Multiresolution Estimation of Parametric Motion Models*, Journal of Visual Communication and Image Representation **6** (1995), 348-365;

[OS] **S. Osher and J. Sethian**, *Fronts Propagating with Curvature Dependent Speed: Algorithms Based on the Hamilton-Jacobi Formulation*, Journal of Computational Physics **79** (1990), 12-49;

[RVW] **B. M. ter Haar Romeny, M. A. Viergerer and J. Weickert**, *Efficient and Reliable Schemes for Nonlinear Diffusion Filtering*, IEEE Trans. Image Proc. (1998);

[SD] **O. Sanchez and F. Dibos**, *Displacement Following of Hidden Objects in a Video Sequence*, International Journal of Computer Vision **57 n° 2** (2004), 91-105;

[SZ] **J. Sokolowski and J.-P. Zolésio**, *Introduction to Shape Optimization. Shape sensitivity analysis*, Springer Ser. Comput. Math., Springer-Verlag (1992);

[WS] **J. Weickert and C. Schnörr**, *Variational Optic flow Computation with a Spatio-Temporal Smoothness Constraint*, Journal of Mathematical Imaging and Vision, Kluwer Academic Publishers **14** (2001), 245-255.